Carbohydrate Polymers 89 (2012) 519–525

Contents lists available at SciVerse ScienceDirect

Carbohydrate Polymers

journal homepage: www.elsevier.com/locate/carbpol

Further analysis of the structure and immunological activity of an RG-I type pectin from *Panax ginseng*

Xu Zhang[a,c,1], Shanshan Li[a,1], Lin Sun[a], Li Ji[a], Jingjing Zhu[a,b], Yuying Fan[a], Guihua Tai[a,b], Yifa Zhou[a,*]

[a] School of Life Sciences, Northeast Normal University, Changchun 130024, PR China
[b] State Key Laboratory of Natural and Biomimetic Drugs, Peking University, Beijing 100191, PR China
[c] College of Life and Environmental Science, Wenzhou University, Wenzhou 325035, PR China

ARTICLE INFO

Article history:
Received 23 December 2011
Received in revised form 14 February 2012
Accepted 13 March 2012
Available online 23 March 2012

Keywords:
Ginseng polysaccharide
Arabinogalactan
RG-I domain
Partial acidic hydrolysis
Immunological activity

ABSTRACT

In this paper, we further analysed the structure of a type I rhamnogalacturonan (RG-I) pectin (WGPA-2-RG) fractionated from ginseng polysaccharides. Methylation and periodate oxidation analyses showed that WGPA-2-RG has a backbone consisting of alternating rhamnose (Rha) and galacturonic acid (GalA) residues and side chains consisting of type II arabinogalactan (AG-II). Partial acidic hydrolysis for 6 h completely removed arabinose (Ara), partial galactose (Gal), but little GalA and Rha. During partial hydrolysis, the molecular weight of WGPA-2-RG decreased smoothly, suggesting that the Ara and cleavable Gal residues exist on the surface of the molecule, while GalA and Rha residues exist in the core of the molecule. The bioactivity assay showed that the arabinogalactan side chains of WGPA-2-RG are essential structures for stimulating NO secretion and lymphocyte proliferation. However, removal of the Ara and Gal residues through hydrolysis did not appreciably affect the ability of WGPA-2-RG to enhance macrophage phagocytosis.

1. Introduction

Panax ginseng C.A. Meyer (ginseng) is a medicinal plant widely used for curing many diseases (Chang, Seo, Gyllenhaal, & Block, 2003; Choi, 2008; Helms, 2004). Ginseng polysaccharides are active compounds that have immunomodulating, antitumour, antiadhesive, antioxidant and hypoglycaemic activities (Kim, Kang, & Kim, 1990; Lee et al., 2006; Luo & Fang, 2008; Shin et al., 2004; Song et al., 2002; Suzuki & Hikino, 1989). Five years ago, we started a research program to systematically study ginseng polysaccharides to obtain more information about the relationship between the structure and activity of ginseng pectin. To date, we have completely fractionated ginseng polysaccharides by a combination of procedures (Zhang et al., 2009) and investigated their structures by enzymatic hydrolysis, NMR and other chemical methods (Yu et al., 2010). We then studied the activities of these fractions, including the inhibitory effects on cell migration (Fan, Cheng, Li, et al., 2010; Fan, Cheng, Liu, et al., 2010), antiproliferative effects on HT-29 human colon cancer cells (Cheng et al., 2011), antitumour and immunomodulatory effects (Ni et al., 2010), antifatigue activity (Wang, Grinberg, et al., 2010) and antidepressant-like effects (Wang, Li, et al., 2010), to better understand the relationships between structure and function in these molecules.

As shown in our previous results (Yu et al., 2010; Zhang et al., 2009) and elsewhere in the literature (Konno, Murakami, Oshima, & Hikino, 1985; Lee et al., 2006; Tomoda, Hirabayashi, et al., 1993; Tomoda, Takeda, et al., 1993), ginseng polysaccharides are mainly composed of starch-like glucans and pectins. In our systematic fractionation, ginseng pectins were separated into type I rhamnogalacturonan (RG-I) and homogalacturonan (HG) groups. The RG-I group pectins were collected in four fractions, WGPA-1-RG ~ 4-RG, where each fraction contained different amounts of the RG-I domains. The HG group was collected in four fractions, WGPA-1-HG ~ 4-HG, where all fractions were primarily composed of the HG domains. Initial structural analysis showed that among the fractions of the RG-I group, WGPA-1-RG contained arabinogalactans (AG) with trace amounts of RG-I domains, WGPA-2-RG contained an AG with minor amounts of RG-I domains, and WGPA-3-RG and WGPA-4-RG contained both RG-I and HG domains. AG and RG-I domains are very complex structures with diverse biological activities. Although we have identified the structural features of the ginseng pectic fractions, less is known about their fine structures. To determine the structure-activity relationship of ginseng pectins, we are beginning to analyse the fine structures of the RG-I group fractions. In this paper, we report the results of our additional analysis of the WGPA-2-RG fraction.

* Corresponding author at: School of Life Sciences, Northeast Normal University, 5268 Renmin Street, Changchun 130024, PR China. Tel.: +86 431 85098212; fax: +86 431 85098212.
E-mail address: Zhouyf383@nenu.edu.cn (Y. Zhou).
[1] These authors contributed equally to this paper.

0144-8617/$ – see front matter © 2012 Elsevier Ltd. All rights reserved.
doi:10.1016/j.carbpol.2012.03.039

2. Materials and methods

2.1. Materials

WGPA-2-RG was prepared by our research group as described in literature (Zhang et al., 2009). All chemicals and reagents were of analytical grade produced in China.

2.2. Analytical methods

Total carbohydrate contents were determined by the phenol–sulphuric acid method (Dubois, Gilles, Hamilton, Rebers, & Smith, 1956). Uronic acid contents were determined by the m-hydroxydiphenyl method (Blumenkrantz & Asboe-Hansen, 1973). All gel permeation and anion exchange chromatographies were monitored by assaying total sugar and uronic acid contents.

Sugar composition analysis was performed as follows. Each polysaccharide sample (2 mg) was hydrolysed with 2 M trifluoroacetic acid (TFA) at 120 °C for 2 h. The released monosaccharides were derivative by 1-phenyl-3-methyl-5-pyrazolone according to literature (Yu et al., 2010) and analysed on a DIKMA Inertsil ODS-3 column (4.6 mm × 150 mm) connected to a Shimadzu high performance liquid chromatography (HPLC) system (LC-10ATvp pump and SPD-10AVD UV-VIS detector).

The molecular weight was estimated by high performance gel permeation chromatography (HPGPC) on a TSK-gel G-3000PW$_{XL}$ column (7.8 mm × 300 mm, TOSOH, Japan) coupled with a Shimadzu HPLC system as described by Zhang et al. (2009). The column was pre-calibrated by standard dextrans (50 kDa, 25 kDa, 12 kDa, 5 kDa and 1 kDa) using linear regression. The sample (20 μL, 5 mg/mL) was injected, eluted with 0.2 M NaCl at a flow rate of 0.6 mL/min and monitored using a refractive index RID-10A detector (Shimadzu, Tokyo, Japan).

2.3. Methylation analysis

The methylation analysis of WGPA-2-RG was performed according to the method described previously (Needs & Selvendran, 1993). The partially methylated alditol acetates were analysed on a gas chromatograph mass spectrometer (GC–MS) (Agilent 6890N-5975) detector. The conditions of GC column were as follows: initial temperature 160 °C for 1 min, then 2 °C/min to 210 °C for 1 min, and then 5 °C/min to 240 °C for 10 min; injection temperature 275 °C. Nitrogen was used as a carrier gas and maintained at 1.0 mL/min. Inositol was used as an internal standard. The percentage of the methylated sugars was estimated as ratios of the peak areas.

2.4. Periodate oxidation and Smith degradation

WGPA-2-RG (20 mg) was dissolved in 0.015 M $NaIO_4$ (50 mL), and kept at 4 °C in dark for 72 h. The reaction was monitored with spectrophotometric method at 223 nm (Dixon & Lipkin, 1954). The $NaIO_4$ consumption was calculated according to the decrease in absorbance at 223 nm. The formic acid production was determined by titration with 0.005 M NaOH. Ethylene glycol was added to decompose the excess $NaIO_4$. The mixture was dialyzed against tap water (24 h) and distilled water (24 h) in turn, and the retentate was reduced with $NaBH_4$ overnight. After neutralization and dialysis, the retentate was freeze-dried, completely hydrolysed, reduced by $NaBH_4$, acetylated and then analysed for sugar composition by gas chromatograph (GC) following the conditions mentioned. The initial column temperature was 170 °C for 2 min, up to 240 °C at 8 °C/min, 240 °C for 1 min, then up to 265 °C at 8 °C/min, 265 °C for 17 min. The injection temperature was 275 °C. Nitrogen was used as a carrier gas and maintained at 1.0 mL/min. Inositol was used as an internal standard.

2.5. Partially acidic hydrolysis

WGPA-2-RG (20 mg) was treated with 0.1 M TFA (2 mL) at 80 °C. After hydrolysis for 0.5, 1, 2,. . .,9 h, the hydrolysate (150 μL) was taken and anhydrous ethanol (1 mL) was added to terminate the reaction, respectively. After removal of TFA by evaporation at 40 °C water bath, the sugar composition and molecular weight of the hydrolysate was analysed by HPGPC as described in the analytical methods above.

The hydrolysates in different hydrolysis times were prepared as follows. WGPA-2-RG (100 mg) was hydrolysed with 0.1 M TFA (5 mL) at 80 °C for 30 min. The hydrolysed product mixture was dialyzed against distilled water to give a remaining polysaccharide fraction RG-0.5H-I (inside of dialysis sack, 82 mg) and the oligomer and monomer mixture RG-0.5H-II (out of dialysis sack). RG-0.5H-I (80 mg) was hydrolysed with 0.1 M TFA (5 mL) at 80 °C for 30 min and the products were treated as described above to give the remaining polymer fraction RG-1H-I (43 mg) and the oligomer and monomer mixture RG-1H-II. RG-1H-I (40 mg) was further hydrolysed with 0.1 M TFA (5 mL) at 80 °C for 5 h, treated as in above, to give the remaining polymer fraction RG-6H-I (23 mg) and the oligomer and monomer mixture RG-6H-II.

2.6. NMR spectra

The ^{13}C NMR spectra were obtained on a Bruker AV600 spectrometer at 150 MHz. The sample (20 mg) was dissolved in D_2O (1 mL, 99.8%) with overnight stirring at room temperature. The spectra were recorded at 25 °C. Acetone was used as an internal standard.

2.7. Immunological activity in vitro

2.7.1. Lymphocyte proliferation assay

Spleens were collected from normal mice under aseptic conditions and minced using forceps through a piece of absorbent gauze in mice lymphocyte separating medium (5 mL). After centrifugation (1500 r/min, 15 min), the supernatant was collected and double diluted to obtain pellets *i.e.* splenocytes. The splenocytes were washed three times in D-Hank's and resuspended in RPMI 1640 complete medium (Gibco), supplemented with 10% new-born calf serum (Gibco), 100 kU/L benzyl penicillin (Hyclone), 100 mg/L streptomycin (Hyclone) and 10 μM HEPES (Sigma), pH 7.2. Splenocytes (100 μL/well, 5×10^6/mL) were seeded in a 96-well plate in the medium with WGPA-2-RG or RG-6H-I (in concentrations 1, 10, 50, 100 and 200 μg/mL), giving a final volume of 200 μL. The plates were incubated at 37 °C, 5% carbon dioxide (CO_2) incubator for 48 h, MTT (20 μL, 5 mg/mL) was added to each well and the plate was incubated for another 4 h. After aspirating the supernatant from the wells, dimethyl sulfoxide (DMSO) (150 μL) was added for dissolution of the formazan crystals. The absorbance at 570 nm was measured using a microplate reader.

2.7.2. Macrophage phagocytosis assay

The macrophages were obtained by peritoneal lavage with D-Hank's from the normal mice. After centrifugation at 1000 r/min for 5 min, the supernatant was discarded, and then the cells were resuspended in RPMI 1640 complete medium. The cells were placed in a flat-bottomed culture plate and incubated at 37 °C for 4 h in 5% CO_2 incubator. The supernatant was isolated and the non-adherent cells were washed out, then the monolayer macrophages were collected.

Phagocytosis of macrophages was measured by neutral red uptake method as described (Ni et al., 2009; Weeks, Keisler, Myrvik, & Warinner, 1987). Briefly, the macrophages were seeded in 96-well plates at a density of 2×10^5 cells/well. The cells were

Table 1
GC–MS analysis of the methylated products of WGPA-2-RG.

Methylated sugars (as alditol acetates)	Type of linkage	Molar ratio	Mass fragments (*m*/*z*)
1,4-Di-O-acetyl-2,3,5-tri-O-methyl-arabinitol	Terminal Ara*f*	19.7	87, 101, 118, 129, 161
1,3,4,5-Tetra-O-acetyl-2-O-methyl-arabinitol	1,3,5-linked Ara*f*	18.1	85, 99, 118, 127, 159, 201, 261
1,4,5-Tri-O-acetyl-2,3-di-O-methyl-arabinitol	1,5-linked Ara*f*	14.6	87, 102, 118, 129, 189
1,5-Di-O-acetyl-2,3,4-tri-O-methyl-arabinitol	Terminal Ara*p*	0.5	101, 117, 161
1,2,5,6-Tetra-O-acetyl-3,4-di-O-methyl-galactitol	1,3,6-linked Gal*p*	20.1	87, 101, 129, 189, 233
1,3,5-Tri-O-acetyl-2,4,6-tri-O-methyl-galactitol	1,3-linked Gal*p*	10.7	101, 118, 129, 161, 234, 277
1,5,6-Tri-O-acetyl-2,3,4-tri-O-methyl-galactitol	1,6-linked Gal*p*	5.9	87, 102, 117, 161, 189, 233
1,5-Di-O-acetyl-2,3,4,6-tetra-O-methyl-galactitol	Terminal Gal*p*	5.7	71, 87, 102, 118, 129, 145, 161, 205
1,2,4,5-Tetra-O-acetyl-3-O-methyl-rhamnitol	1,2,4-linked Rha*p*	3.2	87, 101, 117, 129, 143, 189, 203
1,2,5-Tri-O-acetyl-3,4-di-O-methyl-rhamnitol	1,2-linked Rha*p*	0.7	89, 100, 131, 190, 234, 304
1,5-Di-O-acetyl-2,3,4-tri-O-methyl-rhamnitol	Terminal Rha*p*	0.4	59, 71, 89, 102, 115, 118, 131, 162, 175

incubated in a medium alone, or medium containing various concentrations (1, 10, 50, 100 and 200 μg/mL) of two kinds of polysaccharides or LPS (10.0 μg/mL) as a positive control. The final volume was 200 μL. After 24 h incubation in 5% CO_2 incubator, 0.075% of neutral red dye was added to each well (100 μL/well). The plate was incubated for another 3 h. Then washed three times with PBS (pH 7.2). Finally, 100 μL of cell lysate (0.1 mol/L acetic acid/ethanol 1:1) was added to each well and the plate was placed at room temperature overnight. The absorbance was measured at 540 nm with microplate reader (Olympus CX21, Japan, 100 × objective lens).

2.7.3. Nitrite production assay

The peritoneal macrophages (2.5×10^5 cells/well) were plated in 48-well plates and treated with polysaccharides for 48 h as described above. The supernatants were collected and mixed with an equal volume of Griess reagent (1% sulfanilamide in 2.5% phosphoric acid, 0.1% naphthylethylenediamine dihydrochloride in 2.5% phosphoric acid). After 10 min, absorbance was measured at 540 nm with microplate reader. Sodium nitrite was used to generate a standard curve (Flick & Gifford, 1984; Ruan, Su, Dai, & Wu, 2005).

2.8. Statistical analysis

The results were expressed as the mean ± S.D. of the indicated number of experiments. The data were analysed for significance using the Student's *t* test. *P*-values of <0.05 and <0.01 were considered statistically significant.

3. Results and discussion

The WGPA-2-RG fraction was collected from *P. ginseng* C.A. Meyer as described in our previous work (Zhang et al., 2009). WGPA-2-RG primarily contained galactose (Gal), arabinose (Ara), rhamnose (Rha), and galacturonic acid (GalA) residues in a ratio of 44.4:40.9:4.1:5.3, respectively. The Rha/GalA ratio was 0.77, which falls within the RG-I range of 0.05–1.0, as previously defined by Schols and Voragen (1996) and Yu et al. (2010). Therefore, WGPA-2-RG might contain an RG-I type pectin with arabinogalactan side chains. Its molecular weight was approximately 1.1×10^5 Da.

3.1. Methylation analysis of WGPA-2-RG

Methylation analysis indicated that the Ara residues of WGPA-2-RG existed as terminal, 1,5- and 1,3,5-linked units (Table 1). Among these residues, approximately 38% of the Ara*f* residues were located in terminal positions and 62% occurred in 1,5-linked forms, of which 55% were branched at the O-3 position. A few of the Ara*p* residues were found in terminal positions in WGPA-2-RG, similar to some type II arabinogalactans (AG-II) (Paulsen & Barsett, 2005). As shown in Table 1, four main methylated products of Gal*p* were detected, including 1,3,6- (20.1%), 1,3- (10.7%), 1,6- (5.9%) and terminal (5.7%) linked Gal*p* residues. It was deduced from this result that 1,3-linked Gal*p* in WGPA-2-RG was the main linkage form (72.6%), and of these linkages, 65.3% were branched at the O-6 position. Based on the hypothesis by Paulsen and Barsett (2005), WGPA-2-RG might contain highly branched AG-II with 1,3-linked galactan substituted at O-6 by Gal*p* or Ara*f*. Although Gal*p*A residues cannot be detected by this GC–MS methylation method (Needs & Selvendran, 1993), 1,2- (0.7%) and 1,2,4-linked Rha*p* (3.2%) were detected, which is consistent with the RG-I structural features, where the 1,2-linked Rha*p* residues are partially branched at the O-4 position in the backbone of the RG-I domains. In addition, terminal Rha*p* (0.4%), which is usually present in AG-II, was also detected.

3.2. Periodate oxidation and Smith degradation

WGPA-2-RG was completely oxidised by periodate. On average, 1 mol of glycosyl residue consumed 0.57 mol of periodate; this reaction did not produce formic acid. This result indicated that there were few 1- or 1,6-hexose linkages, which is consistent with the results obtained from the methylation analysis. The Smith degradation products were analysed by GC and HPGPC. GC analysis showed that the products contained glycerol, erythritol, arabinose and galactose. The presence of glycerol and erythritol support the methylation analysis results that showed that WGPA-2-RG contains terminal Ara, terminal Gal, 1,2-linked Rha, 1,6-linked Gal and 1,5-linked Ara. The presence of Ara and Gal in the degradation products confirmed the methylation results that showed that WGPA-2-RG contains 1,3-linked Gal*p*, 1,3,6-linked Gal*p* and 1,3,5-linked Ara*f*. The products of Smith degradation were subjected to HPGPC analysis using a TSK-Gel G3000PW$_{XL}$ column. As shown in Fig. 1, the peak of the molecular weight distribution of the oligosaccharides produced by periodate oxidation occurs at approximately 2000 Da. Sugar analysis indicated that the oligosaccharides produced contained Ara (5.8%), Gal (55.6%), and Rha (5.8%). These results are consistent with the hypothesis that WGPA-2-RG is an

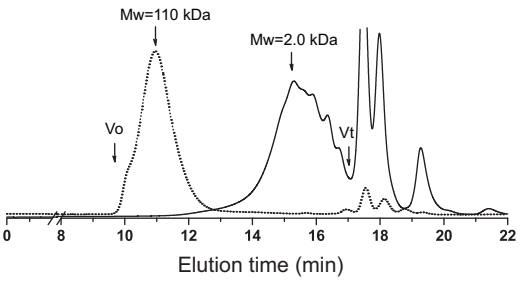

Fig. 1. Molecular weight distributions of WGPA-2-RG and its Smith degradation products as determined by HPGPC (. . ., WGPA-2-RG; —, products of Smith degradation).

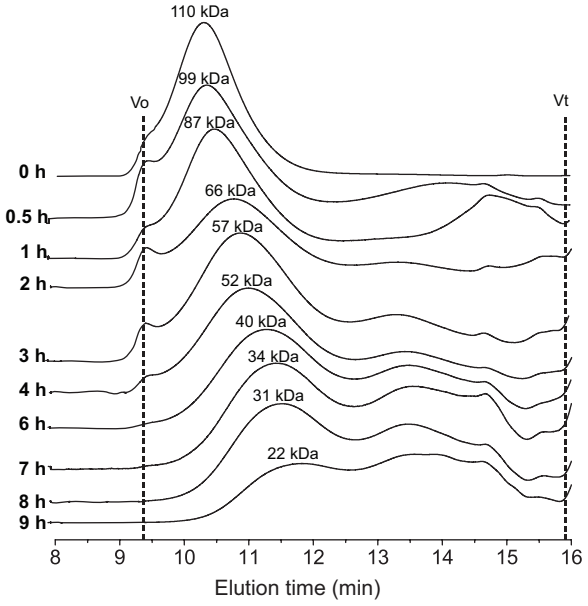

Fig. 2. HPGPC profiles of WGPA-2-RG hydrolysates.

RG-I type pectin. The GalA present in the backbone was oxidised by periodate oxidation to produce the oligosaccharides.

3.3. Partial acid hydrolysis of WGPA-2-RG

WGPA-2-RG was partially hydrolysed using 0.1 M TFA under mild conditions. The hydrolysates arising from different hydrolysis times were analysed by HPGPC. As shown in Fig. 2, WGPA-2-RG was gradually hydrolysed with time, and the molecular weight of the remaining polysaccharide decreased from 110 kDa to 22.7 kDa in a smooth fashion, which indicated that the core structures of WGPA-2-RG were not broken by acid hydrolysis, but the side chains were gradually cleaved.

To investigate the core structures of WGPA-2-RG, the hydrolysates present after 0.5, 1 and 6 h hydrolysis reactions were collected and separated *via* dialysis into two fractions. Fraction I contained the intact core, found in the retentate, and fraction II contained monosaccharides and oligosaccharides, found in the dialysate (Fig. 3). The sugar compositions of these fractions are listed in Table 2. In the remaining polymer, GalA and Rha increased from 5.3 and 4.1% (RG-0.5H-I) to 8.6 and 10.1% (RG-6H-I), respectively; Ara decreased from 40.9 to 0%, whereas Gal increased from 44.4 to 76.1%. The changes in sugar composition of the released

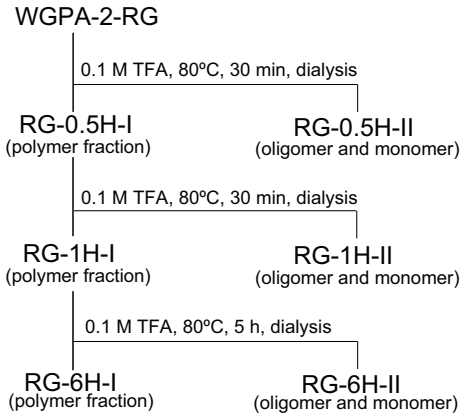

Fig. 3. The procedure used to prepare the hydrolysates of WGPA-2-RG.

Table 2
Sugar composition of WGPA-2-RG and its hydrolysates.

Fraction	Reaction time (h)	Monosaccharide composition (%)					
		Ara	Gal	Glc	Rha	GalA	GlcA
WGPA-2-RG	0	40.9	44.4	2.9	4.1	5.3	2.0
RG-0.5H-I	0.5	30.8	52.8	2.7	5.7	5.5	2.4
RG-1H-I	1	21.2	59.9	2.0	6.9	6.7	3.4
RG-6H-I	6	0.0	76.1	0.6	10.1	8.6	4.6
RG-0.5H-II	0.5	76.2	10.1	2.1	1.2	1.2	0.2
RG-1H-II	1	81.3	14.8	2.7	0.9	0.1	0.2
RG-6H-II	6	42.2	46.8	6.5	0.5	0.8	0.3

mono- and oligomers were found to be consistent with those observed for the remaining polymer. These sugar composition changes indicated that after 6 h of hydrolysis, Ara was completely cleaved, Gal was partially hydrolysed, and little of GalA and Rha were hydrolysed. In the remaining polymer, the amount of Gal increased with the hydrolysis time because Gal was hydrolysed at a slower rate than was Ara. The selective removal of different sugars reflected the different lability of the glycosidic linkages within the RG-I. Complete hydrolysis of Ara and partial hydrolysis of Gal did not cause the dramatic decrease in the molecular weight of WGPA-2-RG, which is consistent with the location of the different sugar residues thus Ara was linked to the surface of the molecule in WGPA-2-RG, whereas Gal was located closer to the core structure (Dong et al., 2010). GalA and Rha were not hydrolysed, which indicated that these probably reside in the core of WGPA-2-RG.

The remaining core structure of WGPA-2-RG after partial hydrolysis was further analysed by NMR. The NMR spectra of WGPA-2-RG and its hydrolysis products are shown in Fig. 4. The major chemical shifts were assigned based on literature values and our composition and structural analysis (Table 3). The anomeric carbon signals of 1,5-linked α-Ara*f*, 1,3,5-linked α-Ara*f* and terminal α-Ara*f* were at 109.19, 107.39 and 107.06 ppm, respectively (Cipriani, Mellinger, Gorin, & Iacomini, 2004). The ratios of these three signals varied among WGPA-2-RG, RG-0.5H-I, RG-1H-I and RG-6H-I and were calculated to be 1.5:1.3:1, 3:1.5:1, 6:2:1 and 0:0:0, respectively. The ratio variation indicated that terminal α-Ara*f* was cleaved first and its presence gradually decreased in the remaining polymers. The hydrolysis of the branched terminal α-Ara*f* at position 3 of 1,3,5-linked α-Ara*f* caused the increase in 1,5-linked α-Ara*f*. Therefore, it was deduced that Ara*f* is located on the surface of the molecules.

Gal gave four anomeric carbon signals at 104.33, 103.11, 102.59 and 102.23 ppm in the spectrum of WGPA-2-RG, representing

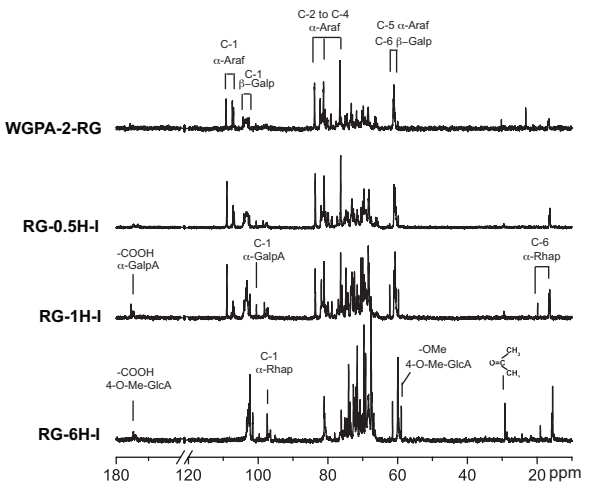

Fig. 4. ^{13}C NMR spectra of WGPA-2-RG and its hydrolysates.

Table 3
Assignments of the major carbon atom signals from WGPA-2-RG and its hydrolysates as determined by ^{13}C NMR.

Residue	Carbon atom	Fractions			
		WGPA-2-RG	RG-0.5H-I	RG-1H-I	RG-6H-I
Arabinose					
1,5-α-Ara*f*	C-1	109.19	108.99	108.39	–
1,3,5-α-Ara*f*	C-1	107.39	106.93	107.20	–
t-α-Ara*f*	C-1	107.06	106.86	106.87	–
t-α-Ara*p*	C-1	–	107.19	107.67	–
Galactose					
t-β-Gal*p*	C-1	104.33	104.10	104.07	103.27
1,3,6-β-Gal*p*	C-1	103.11	103.47	103.51	102.91
1,3-β-Gal*p*	C-1	102.59	103.17	103.18	102.72
1,6-β-Gal*p*	C-1	102.23	102.93	102.94	102.35
Rhamnose					
1,2-α-Rha*p*	C-1	–	98.56	98.21	97.39
1,2,4-α-Rha*p*	C-1	–	97.69	97.48	96.69
1,2-α-Rha*p*	C-6	16.05	16.28	16.35	15.53
1,2,4-α-Rha*p*	C-6	16.55	16.52	16.59	15.78
Galacturonic acid					
1,4-α-Gal*p*A-(1,2-α-Rha*p*)	C-1	–	97.42	97.22	96.48
1,4-α-Gal*p*A-(1,2,4-α-Rha*p*)	C-1	–	100.56	100.49	99.68
1,4-α-Gal*p*A	C-6	175.67	174.59	174.54	174.68
Glucuronic acid					
4-O-Me-Glc*p*A	C-1	–	102.47	102.38	101.57
4-O-Me-Glc*p*A	C-6	176.10	175.49	175.44	175.51
4-O-Me-Glc*p*A	—OMe	59.45	59.80	59.75	58.92
CH_3COO^-		–	–	19.83	19.04

terminal β-Gal*p*, 1,3,6-linked β-Gal*p*, 1,3-linked β-Gal*p* and 1,6-linked β-Gal*p*, respectively (Cipriani et al., 2004). These linkage forms of Gal*p* are typical of AG-II. The variation in these NMR signal intensities for the remaining polymers during hydrolysis indicated that 1,3-linked β-Gal*p* comprises the main chains of AG, while 1,6-linked β-Gal*p* is located on the side chains and is substituted at C-3 by Gal*p* and Ara*f*. Due to either the hydrolysis of Gal*p* or Ara*f* at C-3 on 1,6-linked β-Gal*p*, the amounts of terminal β-Gal*p* and 1,3,6-linked β-Gal*p* decreased rapidly, 1,6-linked β-Gal*p* markedly increased, 1,3-linked β-Gal*p* changed little.

Because the amounts of Rhap and GalpA were relatively low in WGPA-2-RG, their NMR signals were not clearly observed. After acid hydrolysis, the amount of Rha*p* and Gal*p*A increased in the remaining polymer fractions, and thus, the C-1 signals for 1,2-linked α-Rha*p* and 1,2,4-linked α-Rha*p* appeared at 98.56 and 97.69 ppm, respectively, as did their C-6 chemical shifts at 16.28 and 16.52 ppm, respectively (Gorin & Mytosk, 1975). As the time of acid hydrolysis was prolonged, the signal intensities of both C-1 and C-6 for 1,2-linked α-Rha*p* increased, while those of 1,2,4-linked α-Rha*p* decreased, due to the hydrolysis of Gal*p* or Ara*f* substituents at position C-4 of Rha*p*. Correspondingly, the signals of 1,4-linked α-Gal*p*A linked to 1,2-linked α-Rha*p* increased, and the signals of 1,4-linked α-Gal*p*A linked to 1,2,4-linked α-Rha*p* decreased. These results indicate that Rha*p* and Gal*p*A construct the molecular core of WGAP-2-RG.

It has been reported that glucuronic acid (GlcA) usually exists in pectic AG-II domains in its terminal form (Brecker et al., 2005; Ridley, O'Neill, & Mohnen, 2001). As shown in Table 2, the amount of Glc*p*A increased after the acid hydrolysis of WGPA-2-RG. Several NMR signals characteristic of Glc*p*A were observed for the remaining polymer (Table 3). These signals corresponded to the methyl group linked to O-4 of Glc*p*A, C-1 and C-6 of Glc*p*A, which indicated that 4-O-Me-Glc*p*A was present and not cleaved by acidic hydrolysis. This result is similar to the finding that in the arabinogalactan from *Echinacea pallida* (Thude & Classen, 2005), Glc*p*A is at terminal positions and attached to 1,6-linked β-Gal. WGPA-2-RG contained a small amount of glucose (Glc), and this amount decreased gradually in the remaining polysaccharide fractions, suggesting that some Glc*p* is located on the surface of the molecules, possibly linked to Ara*f*. This result is also observed in the arabinogalactan from *E. pallida* (Thude & Classen, 2005).

Summarising the structural analysis results above, it was deduced that WGPA-2-RG is an RG-I type pectin, consisting of a small backbone of alternating Rha and GalA residues, and long AG-II side chains that were linked to the C-4 of the Rha residues. The backbones were cleaved by periodate oxidation, but were not hydrolysed by partial acid hydrolysis. Based on the molecular weight and sugar composition, the backbone was estimated to have approximately 30 repeating units of →4)-Gal*p*A-(1→2)-Rha*p*-(1→, approximately 82% of the Rha residues were substituted by AG-II side chains. The backbones were cleaved by periodate oxidation, but were not hydrolysed by partial acid hydrolysis. The lengths of the AG-II side chains are different, based on the methylation results, their average lengths were estimated to be approximately 25 Gal and Ara residues. Among the Gal and Ara residues, 72.6% of the Gal residues are 1,3-linked forms and comprise the core structures of the AG-II chains, while Ara residues with different linkage forms are linked to the Gal chains and comprise the surface of the molecule. Thus, some of Gal were hydrolysed by partial acid hydrolysis and Ara was completely hydrolysed by the 6 h acid hydrolysis. In addition, small amounts of GlcA and Glc are present at the terminal positions.

3.4. Immunological activities

To investigate the effects of the structural features of WGPA-2-RG on its immunological activities, we tested the activities of WGPA-2-RG and its hydrolysed products on lymphocyte proliferation, macrophage phagocytosis, and nitrite production.

WGPA-2-RG increased lymphocyte proliferation in a dose-dependent manner, as determined by the MTT method, whereas RG-6H-I showed no effect on lymphocyte proliferation (Fig. 5a). The removal of Ara residues resulted in the loss of lymphocyte proliferation activity, suggesting that the Ara in the side chains is important for stimulating lymphocyte proliferation.

The effects of WGPA-2-RG and RG-6H-I on macrophage phagocytosis were tested by measuring the macrophage phagocytosis of neutral red using LPS (10 μg/mL) as a positive control. As shown in Fig. 5b, at a dose of 50 μg/mL, both WGPA-2-RG and RG-6H-I clearly enhanced macrophage phagocytosis. The effects on macrophage phagocytosis were dose dependent, and WGPA-2-RG was found to be slightly more active than RG-6H-I, suggesting that the effects on macrophage phagocytosis do not rely on the Ara side chains.

The peritoneal macrophage production of nitric oxide (NO) was detected by use of a Griess reagent with LPS serving as a positive control (Fig. 5c). The results show that WGPA-2-RG could promote the secretion of NO and this activity was dose dependent for the range of measured concentrations. At a dose of 50 μg/mL, the stimulation of NO production by WGPA-2-RG reached a maximum. However, at this concentration, RG-6H-I lost the ability to stimulate NO production. These results suggest that Ara and AG-II side chains are very important in the stimulation of NO secretion by peritoneal macrophages.

RG-I is one of the primary types of pectin. It is composed of a backbone of alternating α-L-Rha*p* and α-D-Gal*p*A residues. AG is often present in RG-I as side chains (McNeil, Darvill, & Albersheim, 1980). Based on Gal linkage, AG is divided into two types. Type I arabinogalactan (AG-I) consists of a 1,4-linked β-Gal*p* main chain with Ara*f* substituents at O-3. AG-II is, composed of a backbone of 1,3-linked β-Gal substituted at the O-6 position with various combinations of Gal and Ara residues, which is always in the

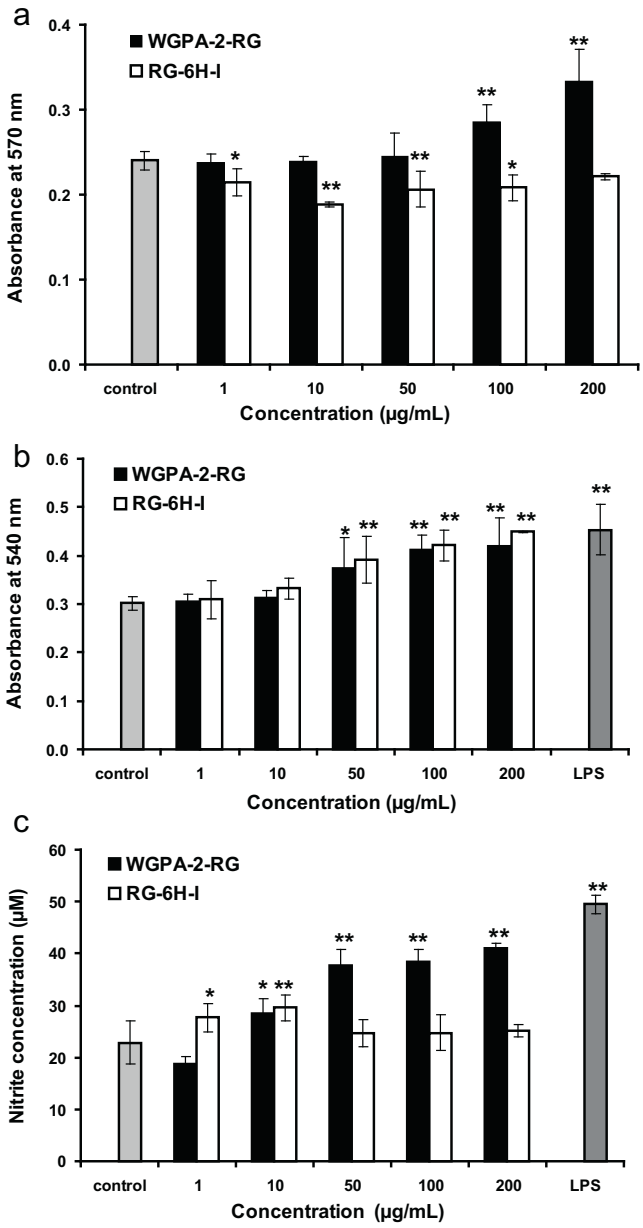

Fig. 5. *In vitro* immunological effects of WGPA-2-RG and RG-6H-I. Each value represents the mean ± S.D. and measured using an ELISA reader. Significant differences from the negative controls were evaluated using Student's *t*-test: $^{*}P < 0.05$, $^{**}P < 0.01$. (a) Lymphocyte proliferation, (b) macrophage phagocytosis, and (c) macrophage NO (as nitrite) production.

form of β-1,6-linked galactan and terminal Ara residues (Serpe & Nothnagel, 1999). Because of its structural complexity, RG-I pectin has many pharmaceutical uses and is an active component of many medicinal plants (Paulsen & Barsett, 2005). As side chains, AG usually plays an important role in these biological activities (Fincher, Stone, & Clarke, 1983).

In this paper, a ginseng pectic fraction, WGPA-2-RG, was analysed and determined to be an RG-I type pectin with a small backbone and long AG-II side chains. WGPA-2-RG was able to stimulate lymphocyte proliferation, macrophage phagocytosis and NO production. The Ara residues linked to the surface of the molecules played a very important role in enhancing lymphocyte proliferation and peritoneal macrophage production of NO, but had less effect on macrophage phagocytosis. Ginseng pectin has been reported to stimulate lymphocyte proliferation, macrophage phagocytosis and NO production (Lim et al., 2002). The experimental results of this paper suggest that WGPA-2-RG contributes to these immunological activities of ginseng pectin.

4. Conclusion

Our structural analysis of WGPA-2-RG indicates that it is an RG-I type pectin with a small backbone of alternating Rha and GalA and long AG-II side chains. The AG-II side chain is a highly branched structure and is attached to the backbone *via* the C-4 of the Rha residues. Most of the Gal residues were determined to be close to the molecular core and Ara on the surface of the molecules. The AG-II chains are composed of 1,3-linked Gal with substituents of Ara and/or Gal at the O-6 positions. 42.9% of the Ara residues are at the non-reducing end of WGPA-2-RG, while the other Ara residues are 1,5- and 1,3,5-linked forms. WGPA-2-RG stimulated lymphocyte proliferation, macrophage phagocytosis, and nitrite production. The removal of Ara residues from WGPA-2-RG decreased its stimulation of lymphocyte proliferation and macrophage nitrite production, but slightly enhanced its macrophage phagocytosis.

Acknowledgments

This work was supported by the National Natural Science Foundation of China (Nos.: 31170770, 30973857, 81173605) and the Fundamental Research Funds for the Central Universities (Structure-anticancer activity relationship of ginseng polysaccharides, No.: 09SSXT125; Studies on fine structures of ginseng pectins, No.: 10SSXT146; Anticancer activity of ginseng pectin and its possible mechanisms, 10QNJJ012).

References

Blumenkrantz, N., & Asboe-Hansen, G. (1973). New method for quantitative determination of uronic acids. *Analytical Biochemistry*, *54*, 484–489.
Brecker, L., Wicklein, D., Moll, H., Fuchs, E. C., Becker, W. M., & Petersen, A. (2005). Structural and immunological properties of arabinogalactan polysaccharides from pollen of timothy grass (*Phleum pratense* L.). *Carbohydrate Research*, *340*, 657–663.
Chang, Y. S., Seo, E. K., Gyllenhaal, C., & Block, K. I. (2003). *Panax ginseng*: A role in cancer therapy? *Integrative Cancer Therapies*, *2*, 13–33.
Cheng, H. R., Li, S. S., Fan, Y. Y., Gao, X. G., Hao, M., Wang, J., et al. (2011). Comparative studies of the antiproliferative effects of ginseng polysaccharides on HT-29 human colon cancer cells. *Medical Oncology*, *28*, 175–181.
Choi, K. T. (2008). Botanical characteristics, pharmacological effects and medicinal compoments of Korean *Panax ginseng* C.A. Meyer. *Acta Pharmacologica Sinica*, *29*, 1109–1118.
Cipriani, T. R., Mellinger, C. G., Gorin, P. A. J., & Iacomini, M. (2004). An arabinogalactan isolated from the medicinal plant *Maytenus ilicifolia*. *Journal of Nature Products*, *67*, 703–706.
Dixon, J. S., & Lipkin, D. (1954). Spectrophotometric determination of vicinal glycols: Application to the determination of ribofuranosides. *Analytical Chemistry*, *26*, 1092–1093.
Dong, Q., Liu, X., Yao, J., Dong, X. T., Ma, C., Xu, Y. X., et al. (2010). Structural characterization of a pectic polysaccharide from *Nerium indicum* flowers. *Phytochemistry*, *71*, 1430–1437.
Dubois, M., Gilles, K. A., Hamilton, J. K., Rebers, P. A., & Smith, F. (1956). Colorimetric method for determination of sugars and related substances. *Analytical Chemistry*, *28*, 350–356.
Fan, Y. Y., Cheng, H. R., Li, S. S., Wang, J., Liu, D., Hao, M., et al. (2010). Relationship of the inhibition of cell migration with the structure of ginseng pectic polysaccharides. *Carbohydrate Polymers*, *81*, 340–347.
Fan, Y. Y., Cheng, H. R., Liu, D., Zhang, X., Wang, B., Sun, L., et al. (2010). The inhibitory effect of ginseng pectin on L-929 cell migration. *Archives of Pharmacal Research*, *33*, 681–689.
Fincher, G. B., Stone, B. A., & Clarke, A. E. (1983). Arabinogalactan-proteins: Structure, biosynthesis and function. *Annual Review of Plant Physiology*, *34*, 47–70.
Flick, D. A., & Gifford, G. E. (1984). Comparison of *in vitro* cell cytotoxic assays for tumor necrosis factor. *Journal of Immunological Methods*, *68*, 167–175.
Gorin, P. A. J., & Mytosk, M. (1975). Further studies on the assignment of signals in ^{13}C magnetic resonance spectra of aldose and derived methyl glycosides. *Canadian Journal of Chemistry*, *53*, 1212–1223.
Helms, S. (2004). Cancer prevention and therapeutics: *Panax ginseng*. *Alternative Medicine Review*, *9*, 259–274.
Kim, Y. S., Kang, K. S., & Kim, S. I. (1990). Study on antitumor and immunomodulating activities of polysaccharide fractions from *Panax ginseng*: Comparison of effects

of neutral and acidic polysaccharide fraction. *Archives of Pharmacal Research*, *13*, 330–337.

Konno, C., Murakami, M., Oshima, Y., & Hikino, H. (1985). Isolation and hypoglycemic activity of Panaxans Q, R, S, T and U, glycans of *Panax ginseng* roots. *Journal of Ethnopharmacology*, *14*, 69–74.

Lee, J. H., Shim, J. S., Lee, J. S., Kim, M. K., Chung, M. S., & Kim, K. H. (2006). Pectin-like acidic polysaccharide from *Panax ginseng* with selective antiadhesive activity against pathogenic bacteria. *Carbohydrate Research*, *341*, 1154–1163.

Lim, D. S., Bae, K. G., Jung, I. S., Kim, C. H., Yun, Y. S., & Song, J. Y. (2002). Anti-septicaemic effect of polysaccharide from *Panax ginseng* by macrophage activation. *Journal of Infection*, *45*, 32–38.

Luo, D., & Fang, B. (2008). Structural identification of ginseng polysaccharides and testing of their antioxidant activities. *Carbohydrate Polymers*, *72*, 376–381.

McNeil, M., Darvill, A. G., & Albersheim, P. (1980). Structure of plant cell walls. X. Rhamnogalacturonan I, a structurally complex pectic polysaccharide in the walls of suspension-cultured sycamore cells. *Plant Physiology*, *66*, 1128–1134.

Needs, P. W., & Selvendran, R. R. (1993). Avoiding ocidative degradation during sodium hydroxide/methyl iodide-mediated carbohydrate methylation in dimethyl sulfoxide. *Carbohydrate Research*, *245*, 1–10.

Ni, W. H., Zhang, X., Bi, H. T., Iteku, J., Ji, L., Sun, C. X., et al. (2009). Preparation of a glucan from the roots of *Rubus crataegifolius* Bge. and its immunological activity. *Carbohydrate Research*, *344*, 2512–2518.

Ni, W. H., Zhang, X., Wang, B., Chen, Y., Han, H., Fan, Y. Y., et al. (2010). Antitumor activities and immunomodulatory effects of ginseng neutral polysaccharides in combination with 5-fluorouracil. *Journal of Medicinal Food*, *13*(2), 1–8.

Paulsen, B. S., & Barsett, H. (2005). Bioactive pectic polysaccharides. *Advances in Polymer Science*, *186*, 69–101.

Ridley, B. L., O'Neill, M. A., & Mohnen, D. (2001). Pectins: structure, biosynthesis, and oligogalacturonide-related signaling. *Phytochemistry*, *57*, 929–967.

Ruan, Z., Su, J., Dai, H. C., & Wu, M. C. (2005). Characterization and immunomodulating activities of polysaccharide from *Lentinus edodes*. *International Immunopharmacology*, *5*, 811–820.

Schols, H. A., & Voragen, A. G. J. (1996). Complex pectins: Structure elucidation using enzymes. *Progress in Biotechnology*, *14*, 3–19.

Serpe, M. D., & Nothnagel, E. A. (1999). Arabinogalactan-proteins in the multiple domains of the plant cell surface. *Advances in Botanical Research*, *30*, 207–289.

Shin, M. J., Kim, Y. S., Kwak, Y. S., Song, Y. B., Kim, Y. S., & Park, J. D. (2004). Enhancement of antitumor effects of paclitaxel (taxol) in combination with red ginseng acidic polysaccharide (RGAP). *Planta Medica*, *70*, 1033–1038.

Song, J. Y., Han, S. K., Son, E. H., Pyo, S. N., Yun, Y. S., & Yi, S. Y. (2002). Induction of secretory and tumoricidal activities in peritoneal macrophages by ginsan. *International Immunopharmacology*, *2*, 857–865.

Suzuki, Y., & Hikino, H. (1989). Mechanisms of hypoglycemic activity of Panaxans A and B, glycans of *Panax ginseng* roots: Effects on the key enzymes of glucose metabolism in the liver of mice. *Phototherapy Research*, *3*, 15–19.

Thude, S., & Classen, B. (2005). High molecular weight constituents from roots of *Echinacea pallida*: An arabinogalactan-protein and an Arabinan. *Phytochemistry*, *66*, 1026–1032.

Tomoda, M., Hirabayashi, K., Shimizu, N., Gonda, R., Ohara, N., & Takada, K. (1993). Characterization of two novel polysaccharides having immunological activities from the root of *Panax ginseng*. *Biological and Pharmaceutical Bulletin*, *16*, 1087–1090.

Tomoda, M., Takeda, K., Shimizu, N., Gonda, R., Ohara, N., Takada, K., et al. (1993). Characterization of two acidic polysaccharides having immunological activities from the root of *Panax ginseng*. *Biological and Pharmaceutical Bulletin*, *16*, 22–25.

Wang, J., Grinberg, S. F., Li, S. S., Liu, H. B., Sun, L., Zhou, Y. F., et al. (2010). Antidepressant-like effects of the active acidic polysaccharide portion of ginseng in mice. *Journal of Ethnopharmacology*, *132*, 65–69.

Wang, J., Li, S. S., Fan, Y. Y., Chen, Y., Liu, D., Cheng, H. R., et al. (2010). Anti-fatigue activity of neutral and acidic polysaccharides from *Panax ginseng* C.A. Meyer. *Journal of Ethnopharmacology*, *130*(2), 421–423.

Weeks, B. A., Keisler, A. S., Myrvik, Q. N., & Warinner, J. E. (1987). Differential uptake of neutral red by macrophages from three species of estuarine fish. *Developmental and Comparative Immunology*, *11*, 117–124.

Yu, L., Zhang, X., Li, S. S., Liu, X. Y., Sun, L., Liu, H. B., et al. (2010). Rhamnogalacturonan I domains from ginseng pectin. *Carbohydrate Polymers*, *79*, 811–817.

Zhang, X., Yu, L., Bi, H. T., Li, X. H., Ni, W. H., Han, H., et al. (2009). Total fractionation and characterization of the water-soluble polysaccharides isolated from *Panax ginseng* C.A. Meyer. *Carbohydrate Polymers*, *77*, 544–552.